Chiang Mai J. Sci. 2018; 45(4) : 1728-1744
http://epg.science.cmu.ac.th/ejournal/
Contributed Paper

Characterization and Expression Analysis of the STAT Pathway in *Anopheles dirus*

Jonathan Wee Kent Liew, Cherng Shii Leong, Meng Li Wong, Indra Vythilingam, Mun Yik Fong and Yee Ling Lau*

Department of Parasitology, Faculty of Medicine, University of Malaya, 50603 Kuala Lumpur, Malaysia.

* Author for correspondence; e-mail: lauyeeling@um.edu.my

Received: 11 May 2017
Accepted: 4 July 2017

ABSTRACT

The Janus kinase-signal transducers and activators of transcription (JAK-STAT) pathway is one of the main signaling pathways mediating immune responses towards malaria parasites in *Anopheles*. Core components of the STAT pathway are STAT, suppressor of cytokine signaling (SOCS) protein, and protein inhibitor of activated STAT (PIAS) protein. However, this pathway is the least studied among the three major signaling pathways. Recent study found that *Anopheles dirus* lacks a second intronless STAT. The implication of this phenomenon is still unclear. Moreover, molecular understanding of *An. dirus* is scarce. Thus, the three components of the pathway were studied using an *Anopheles dirus*/*Plasmodium berghei* experimental model. The three proteins were sequenced and characterized. The STAT, PIAS and SOCS proteins exhibited high sequence similarity with those of other *Anopheles*. Nonetheless, there were no significant changes in the expression levels of the genes post *Plasmodium berghei* infection. The current study warrants further investigation on the JAK-STAT pathway in *Anopheles*. More investigations on the *Anopheles* spp. in different geographical regions should be pursued, to understand the possible differences in the JAK-STAT pathway among these *Anopheles*.

Keywords: *Anopheles dirus*, *Plasmodium berghei*, STAT, PIAS, SOCS, experimental model

1. INTRODUCTION

During the *Plasmodium*'s development in the *Anopheles* mosquito, parasite numbers are suppressed, indicating a robust immune response taking place to combat infection. This innate immune response is mediated by the immune signaling pathways of the mosquito. Among others, the three major and relatively well-characterized pathways are the Toll, immune deficiency (Imd) and Janus kinase-signal transducers and activators of transcription (JAK-STAT) pathways [1]. While the *Anopheles* Toll and Imd pathways are potent and found to regulate effective anti-*Plasmodium* immune factors, the JAK-STAT pathway is not as extensively studied [2].

Besides playing an immunological role, the JAK-STAT pathway mediates gender

determination, cell movement, hematopoesis, cell differentiation, embryonic segmentation and others. The major components of the pathway include the JAK kinase which transmits signals from external stimuli to, the STAT transcription factors, the suppressor of cytokine signaling (SOCS) repressor protein which is part of the negative feedback loop of the pathway and the protein inhibitor of activated STAT (PIAS) repressor protein [3, 4]. The STAT pathway also regulates gene expressions of *SOCS,* nitric oxide synthase (*NOS*) and thioester-containing protein 1 (*TEP1*) [5]. The NOS and TEP1 are highly effective anti-*Plasmodium* immune factors. Thus, the pathway is a potential target for development of malaria control strategies [6]. Yet, the role of the STAT pathway in many other *Anopheles* is not clear. An intronless STAT-B (or STAT1) was uncovered in some subgenera of *Anopheles* but not in *An. dirus*, *An. sinensis*, *An. albimanus*, *An. darlingi* and *An. farauti* [5, 7]. It is unknown if this phenomenon affects the STAT-mediated signaling in these species.

Furthermore, most studies employ *An. gambiae* (an African *Anopheles*) and *An. stephensi* as a model, so the use of other native, primary malaria vectors is scarce, especially those of the South and Southeast Asia regions. The *An. minimus* complex, *An. dirus* complex, *An. leucosphyrus* complex and *An. maculatus* group are some of the principal malaria vectors in these regions with active malaria transmission [8]. It is imperative that the molecular understanding of *Anopheles* immune response be extended to vectors in these malaria endemic regions. The *An. dirus* complex comprises 7 species [9]. Of them, *An. dirus* A is known to occur in Myanmar, Thailand, Cambodia, Laos, Vietnam and Hainan Island [10]. It is an efficient vector known to harbor all human malaria parasites [11-14].

There is little molecular understanding of immune response in *An. dirus*. Previously, we have described the Relish 2 (Rel2) transcription factor of the Imd pathway in *An. dirus* [15]. Therefore, the current study aims to characterize *An. dirus* STAT (AdSTAT), PIAS (AdPIAS) and SOCS (AdSOCS) proteins of the STAT pathway and to study the time-point expression profiles of the genes in the *An. dirus*/*P.berghei* experimental model.

2. MATERIALS AND METHODS

2.1 Animal Use and Ethical Clearance

Laboratory-bred colony of *An. dirus* WRAIR2 strain and *P. berghei* ANKA (MR4/BEI resources) were used in this study. *Plasmodium berghei* infections were also performed on BALB/c female mouse. The Animal Use Protocol (Ethics Reference no.: 20150407/PARA/R/MBK) was approved by the Faculty of Medicine Institutional Animal Care and Use Committee, University of Malaya, Malaysia.

2.2 Rapid Amplification of cDNA Ends (RACE) PCR of *AdSTAT*, *AdSOCS* and *AdPIAS*

2.2.1 PCR using degenerate primers to obtain partial sequences

The genome sequence of *An. dirus* was not available during the time of this study (2013-2014). Degenerate primers (Table 1) were designed on regions with high similarities, based on aligned sequences of the genes of *Anopheles*, *Aedes* and *Culex*, which are available in GenBank. The annealing temperatures for the primers are 50.4°C (STAT), 48.3°C (SOCS) and 43.7°C (PIAS). PCR was performed using GoTaq® Flexi DNA polymerase and mosquito genomic DNA as template. The cycling conditions are 95°C for 5 min; 35 cycles of 94°C for 30 s, annealing for 30 s and extension at 72°C

for 1 min; and a final extension step at 72°C for 10 min. Amplicons were cloned into pGEM®-T Vector (Promega, Madison, USA) and sequenced.

2.2.2 RACE PCR to obtain full-length coding sequences

With the partial sequences obtained from degenerate PCR, RACE PCR primers were designed based on the analyzed partial sequences which constitutes only the exons. Total RNA extraction of whole mosquito and RACE PCR were performed as per previously described [15], using ReliaPrep™ RNA Tissue Miniprep System (Promega, Madison, USA) and SMARTer™ RACE cDNA Amplification kit (Clontech, California, USA). Nested RACE PCR was performed according to the manufacturer's instructions. The primers used for RACE PCR are shown in Table 1.

Table 1. Primers used in PCR.

Primer Sequence (5' to 3')	Annealing temperature (°C)	GenBank accession no. of sequences which primers were designed upon	Expected size (bp)
Degenerate PCR			
STAT STAT-F1: ATGTCACTGTGGGCCCGG STAT-R1: GGCTGCTTCTCGATGATGAA	50.4	FJ792607 AY299687 EF175868	
SOCS SOCSF2: CAGGTCGACTTYATYCACTG SOCSR2: CGRTAGTGGTACTCTTTCAGG	48.3	XM_001844773 EF631979 XM_001656017	-
PIAS PIASD2F1: GRTTYTGYCTGCTRGARAC PIASD-R: GTRCTCCABGAWCCRTCYTT	43.7	HM851177 XM_001688417 XM_001647765 XM_001850599	
RACE PCR*			
STAT GSP1 AdStat5Ra: CTGGTTGTGGCCGTGCGCCCGCATCTC	70.2		

Table 1. Continued.

Primer Sequence (5' to 3')	Annealing temperature (°C)	GenBank accession no. of sequences which primers were designed upon	Expected size (bp)
NGSP1 Ad5RaSTATN1: GCGCCCGGTTCTTCTGCAGCTGTCACC	68.7		
GSP2 AdStat3Ra: GTGCAGGACCCGGAGGTGACGGAGGTG	70.2		-
NGSP2 Ad3RaSTATN2: CGTGCAGGACCCGGAGGTGACGGAGGTG	71.3		
SOCS GSP1 Ad5RaSOCS1: GCTCACAATCACGGCCCGGCACAGCTGC	69.9		
NGSP1 Ad5RaSOCSN1: ACCGTCGACGCCGTAAACACGCCCGG	70.2		
GSP2 Ad3RaSOCS2: GGGGCAAGATGGACCGGTACGAGGCGGAG	70.9	-	
NGSP2 Ad3RaSOCSN2: GGGTACGTTCCTGTTGCGCGACTCGGCC	69.9		
PIAS GSP1 Ad5RaPIAS1: CCCTGGTGTAGTCGGCCGCTTTGACGCC	69.9		
NGSP1 Ad5RaPIASN1: GACGTCAGCTTACGCACCAGGTAGCAGGC	68.1		
GSP2 Ad3RaPIAS2: GCGTGGAACCAAAGAGACCGCCGCGACC	69		
NGSP2 Ad3RaPIASN2: GGTCGCTAACCACATCGCGGTGTCCTGG	67		

Table 1. Primers used in PCR.

Primer Sequence (5' to 3')	Annealing temperature (°C)	GenBank accession no. of sequences which primers were designed upon	Expected size (bp)
qRT-PCR		KX870845	
STAT			113
AdrtSTATF1: CCCGCAACAAGAACTACAT		KX870847	
AdrtSTATR1: CGGTGACTGGATGTTGTAAG			
SOCS			130
AdrtSOCSF3: AATCGCAACTTCAGCTTCA		KX870846	
AdrtSOCSR3: GGTAGTGGTACTCCTTCAGATA			
PIAS			127
AdrtPIASF2: AGGAAGGCTCGTTCTACTT		KY022437	
AdrtPIASR2: TCCAGCAGACAGAATCGTA	57.6		
EF1			118
AdrtEF1F1: CCGGACATCGTGATTTCAT		KY022436	
AdrtEF1R1: TGGCCGTTCTTGGAGATA			
Act			130
AdrtACTF2: TCTGACCGACTACCTGAT		AY369135.2	
AdrtACTR2: CATCTCCTGCTCGAAGTC			
S7			132
AdrtS7F1: GAGGTCGAGTTCAACAACAA			
AdrtS7R1: GAACACGACGTGCTTACC			

*Melting temperature instead of annealing temperature is stated for each RACE primer.

2.3 Molecular and Phylogenetic Analysis of *AdSTAT*, *AdSOCS* and *AdPIAS*

The sequenced products of the 5'-RACE and 3'-RACE PCR for each gene were analyzed and combined to form a consensus sequence using BioEdit Sequence Alignment Editor v7.2.3. BLAST programs were used to analyze and compare the sequences with those in the NCBI database. Results from BLAST and AUGUSTUS (http://bioinf.uni-greifswald.de/augustus/submission), an online gene prediction software were used to estimate the start and stop codon of the genes. Exon/intron boundaries were predicted using AUGUSTUS, GENSCAN (http://genes.mit.edu/GENSCAN.html) and by comparing the sequences with those annotated from other insects. The *An. dirus* whole genome shotgun sequences were used as queries in this case. The proteins were then analyzed for putative conserved domains, using BLASTP and Pfam (http://pfam.xfam.org/). Available STAT, SOCS and PIAS sequences of several insects were obtained from NCBI and aligned using Clustal Omega. Then phylogenetic trees were constructed from these gene sequences using the neighbor-joining method with Jukes-Cantor model (bootstrap value = 1000) in MEGA 7.0.21 software. The *AdSTAT*, *AdPIAS* and *AdSOCS* sequences obtained, were submitted to GenBank with accession numbers KX870845 - KX870847.

2.4 *Plasmodium* Infection of *An. dirus* Mosquitoes

Five- to seven-day old female *An. dirus* WRAIR2 mosquitoes were starved for 2 nights prior to feeding on a *P. berghei* ANKA-infected BALB/c female mouse. Engorged mosquitoes were kept at 20 ± 1°C, 80% humidity. The midguts and salivary glands of the mosquitoes were dissected on Day 10 and starting Day 14 post infection (PI) respectively, for oocyst count and sporozoite observation. Female mosquitoes fed on healthy mouse were used as controls.

2.5 Quantitative Real Time-PCR (qRT-PCR) of *AdSTAT*, *AdSOCS* and *AdPIAS* Post Infection

Four replicates were performed to study the gene expressions of *AdSTAT*, *AdPIAS* and *AdSOCS* at different time points (12 h, 24 h, 48 h and Day 5) post infectious blood meal. All infected mosquitoes used in these experiments took blood meals from mice with parasitemia levels of 5.9 - 6.4% at Day 3 - 4 post *P. berghei* ANKA infection. All fully engorged mosquitoes which fed on such levels of parasites have been found to be 100% infected with oocysts in their midguts. Total RNA from pooled whole mosquitoes were extracted at 12 h, 24 h, 48 h and Day 5 PI. cDNA was synthesized using the qPCRBIO cDNA synthesis kit (PCR Biosystems, London, UK). PCR conditions were the same for all primers (Table 1) i.e. initial denaturation at 95°C for 30 s, followed by 40 cycles of denaturation at 95°C for 10 s and annealing/extension at 57.6°C for 25 s; and finally, a melt curve step from 65-95°C, with increment of 0.5°C every 5 s. qPCR was performed using SsoAdvanced™ Universal SYBR® Green Supermix (Bio-Rad, California, USA) on Bio-Rad CFX96™ Real-Time System. Final concentration of primers in a 20 µL reaction was 312.5 nM. Results of the PCR were analyzed by the Bio-Rad CFX Manager™ 3.1 software. Expression levels were normalized against those of three reference genes i.e. elongation factor 1-alpha, actin 1 and ribosomal protein S7. The $2^{-\Delta\Delta C}{}_{T}$ method was used to calculate the relative expression compared to the controls.

2.6 Statistical Analysis

One-way ANOVA with multiple comparisons of Tukey were used in the analyses. All tests were performed at 95% confidence intervals (alpha = 0.05). The graphs and statistical analyses were accomplished using GraphPad Prism version 5.01.

3. RESULTS AND DISCUSSION

3.1 Molecular and Phylogenetic Analyses of AdSTAT, AdPIAS and AdSOCS Proteins

The length of *AdSTAT, AdPIAS* and *AdSOCS* coding regions are shown in Table 2. The current study found that the length of *AdPIAS* coding sequence is 2004 bp, 141 bp longer than that annotated *in silico* [16]. Multiple sequence alignment confirmed this finding (Figure 1). BLASTN result showed that *AdSTAT*, *AdPIAS* and *AdSOCS* are 99% similar to *An. dirus* strain WRAIR2 whole genome shotgun (WGS) sequence contig 1.3648, contig 1.2776 and contig 1.2079 (GenBank accession: APCL01003649.1, APCL01002777.1 and APCL01002080.1), respectively. Conserved domains typical to each protein of *An. dirus* were detected (Figure 2a). Furthermore, there are seven, ten and three exons on *AdSTAT*, *AdPIAS* and *AdSOCS* genes, respectively (Figure 2b). The AdSTAT, AdSOCS and AdPIAS proteins show high similarities to those of the other Anophelines, and to an extent with *Aedes* and *Culex* (Table 3). Multiple sequence alignments of the protein sequences from Table 3 were performed (Figure 1). Obviously, regions with detected conserved domains exhibit similar amino acid motifs with those of the other insects e.g. C-terminal of the AdSOCS protein. Outside of these, the amino acid sequences demonstrate variability (Figure 1). Among the three proteins, more variations can be observed in the PIAS protein sequences of the Anophelines. The N- and C-terminal of the PIAS proteins are different among the insects, except for the regions where the PINIT and the zinc finger domains are situated. Components of the JAK-STAT pathway are conserved throughout evolution [17]. These results show that those of a Southeast Asian Anopheline are no different.

Table 2. Coding DNA sequence length and protein length of genes sequenced in this study.

	Total base pairs (bp)	Protein length (amino acids)	GenBank accession number	Isoelectric point*	Molecular weight (Dalton)*
STAT	2259	752	KX870845	6.21	86478.59
PIAS	2004	667	KX870846	7.91	72188.60
SOCS	1185	394	KX870847	6.89	42972.67

* predicted by ExPASy Compute pI/Mw tool

a) STAT

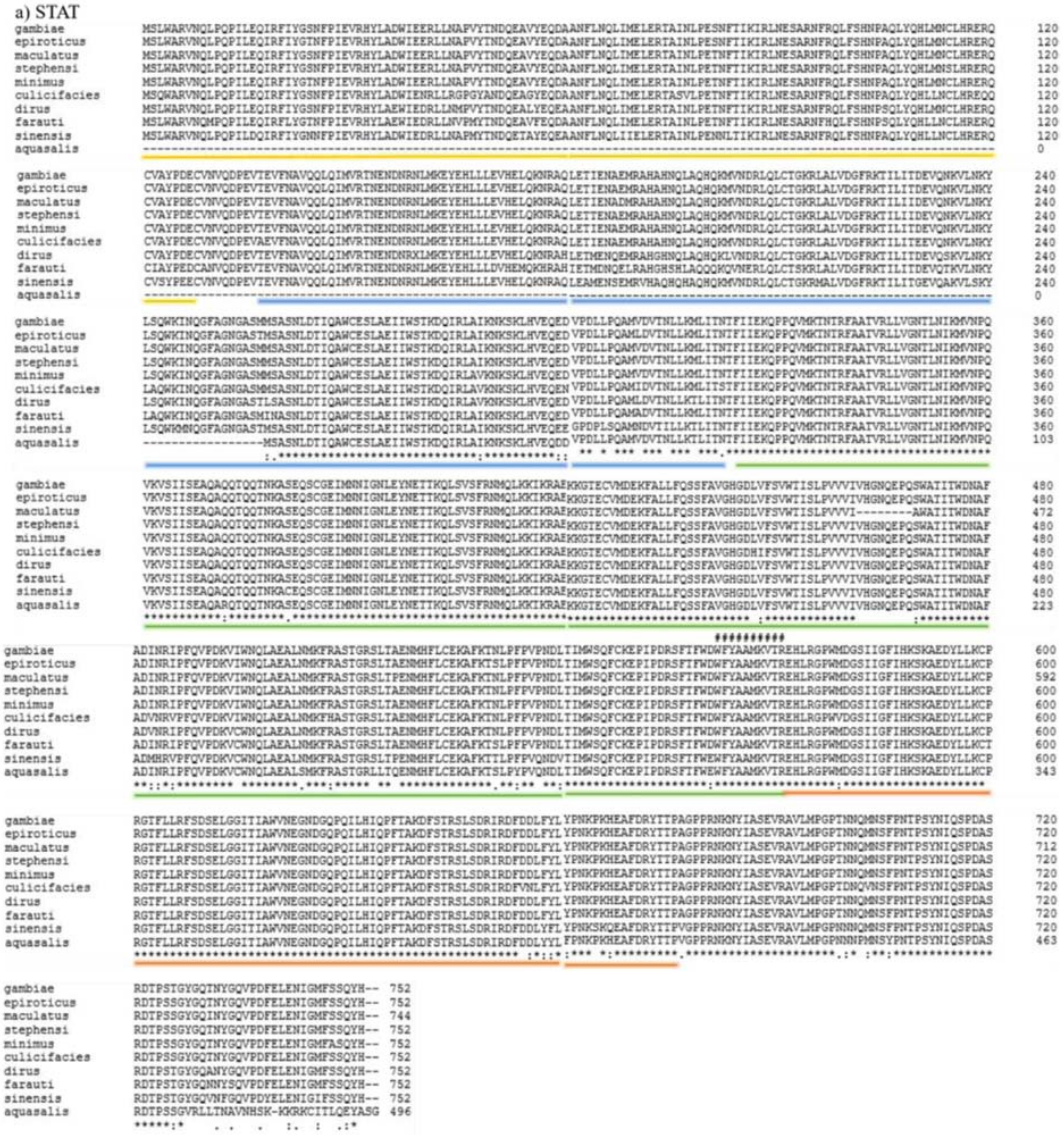
gambiae
epiroticus
maculatus
stephensi
minimus
culicifacies
dirus
farauti
sinensis
aquasalis

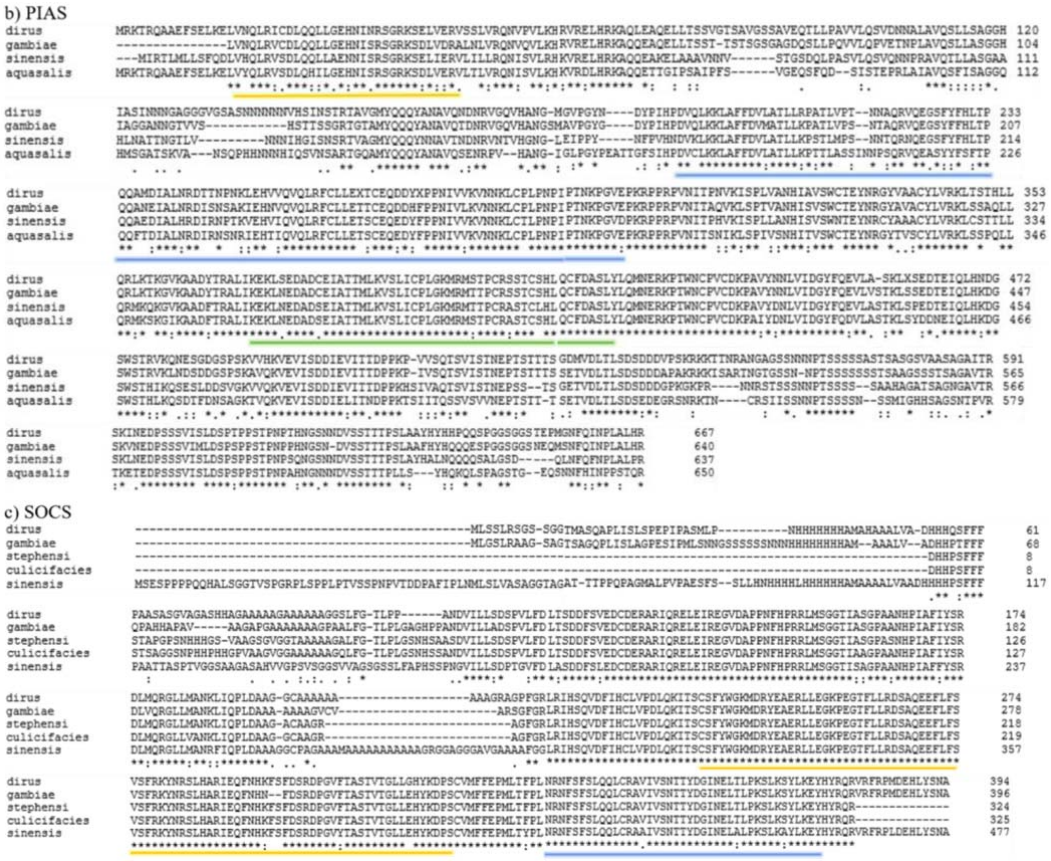

Figure 1. *Anopheles* protein sequences alignments performed using Clustal Omega. Positions which have a single, fully conserved residue are marked *; positions which shows conservation between groups of strongly similar properties are marked (:); positions which shows conservation between groups of weakly similar properties are marked (.). a) STAT protein alignment. Yellow underline - STAT protein interaction domain; blue underline - STAT alpha domain; green underline - STAT DNA binding domain; red underline - SH2 domain; (#) overlapping region of STAT DNA binding domain and SH2 domain. b) PIAS protein alignment. Yellow underline - SAP domain; blue underline - PINIT domain; green underline - MIZ-zing finger domain. c) SOCS protein alignment. Yellow underline - SH2 domain; blue underline - SOCS box. The GenBank accession numbers of the protein sequences used to perform these alignments are those stated in Table 3.

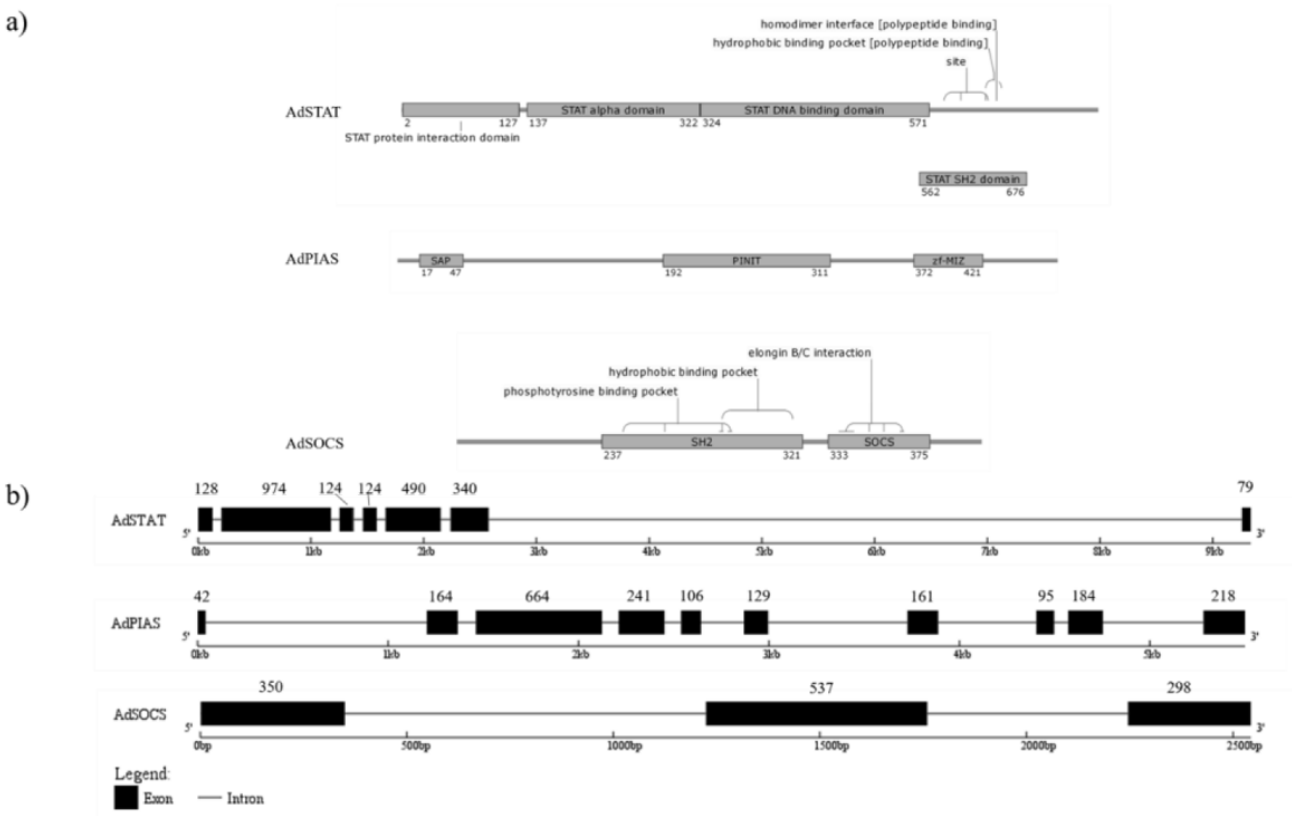

Figure 2. Structural architecture of AdSTAT, AdPIAS and AdSOCS. a) Putative conserved domains detected by Pfam and BLASTP. The numbers denote the region of the domains on the protein sequence. The diagrams are not drawn to scale. SH2 - Src Homology 2; SAP - scaffold attachment factor-A/B, acinus and PIAS; PINIT - Pro-Ile-Asn-Ile-Thr; zf-MIZ - MIZ/SP-RING zinc finger domain with small ubiquitin-like modifier (SUMO) ligase activity; and SOCS - SOCS box. b) Exon/intron boundaries of the genes. The numbers above the exons denote the number of base pairs per exon.

Table 3. Percentage similarity of AdSTAT, AdPIAS and AdSOCS protein sequence to those of other organisms, calculated by Clustal Omega.

Organism	GenBank Accession no.	% Identity
STAT		
AdSTAT	KX870845	
An. dirus	APCL01003649	99.00*
An. gambiae	ACO05014	97.07
An. minimus	DAA79934	96.94
An. epiroticus	DAA79936	96.94
An. stephensi	AKR71985	96.81
An. maculatus	DAA79925	96.51
An. farauti	DAA79938	94.68
An. culicifacies	DAA79933	94.41
An. sinensis	DAA79926	92.55
An. aquasalis	AEK26395	91.30
Ae. aegypti	XP_001653947	79.54
Cx. quinquefasciatus	XP_001866607	77.66
D. melanogaster	NP_732517	41.07
PIAS	KX870846	
AdPIAS	APCL01002777	99.00*
An. dirus	XP_001688469	83.07
An. gambiae	KFB48342	73.23
An. sinensis	AEK26394	68.54
An. aquasalis	XP_001647816	71.74
Ae. aegypti	XP_001850651	68.35
Cx. quinquefasciatus	NP_001286228	54.19
D. melanogaster		
SOCS		
AdSOCS	KX870847	
An. dirus	APCL01002080	99.00*
An. stephensi	AMA22609	87.31
An. culicifacies	AII72405	86.42
An. gambiae	ABV01933	83.51
An. sinensis	KFB35251	75.89
Ae. aegypti	XP_001656067	83.33
Cx. quinquefasciatus	XP_001844825	48.52
D. melanogaster	NP_724096	44.74

*Percentage identity of the cds to the WGS sequence of *An. dirus*.

Studies have uncovered an intronless STATB (or STAT1) as a result of a gene retrotransposition event [5, 7], which is not found in *An. dirus*. This gene duplication occurred after *An. dirus* and *An. farauti* diverged from the other Anophelines of the subgenus *Cellia* [18]. The three genes investigated here diverged long ago from *Drosophila* while the genes of Anophelines are evolutionarily close to those of *Aedes* and *Culex* (Figure 3a-c). Nonetheless, the proteins of the Anophelines diverged from those

of *Aedes*, *Culex* and *Drosophila* and form their own distinct clades (Figure 3a-c). *Anopheles dirus*. The STAT, PIAS and SOCS of Anophelines demonstrate similar patterns of diversification, corroborating results by Gupta (2016). AdSTAT, AdPIAS and AdSOCS are evolutionarily closest to *An. farauti* STAT, *An. gambiae* PIAS and SOCS, respectively. Although the structures and molecular characterization of these proteins have been discussed [7, 16, 19], *STAT* of *An. aquasalis* which lacks the STAT protein interaction domain and half of the STAT alpha domain [6] was rarely included in the analyses. Here, it was found to be closest in evolution to *An. sinensis* (Figure 3a). Nonetheless, all the three genes of the Anophelines evolved and arose temporally close to each other, which may explain the sequence similarity of the proteins within the *Anopheles* group.

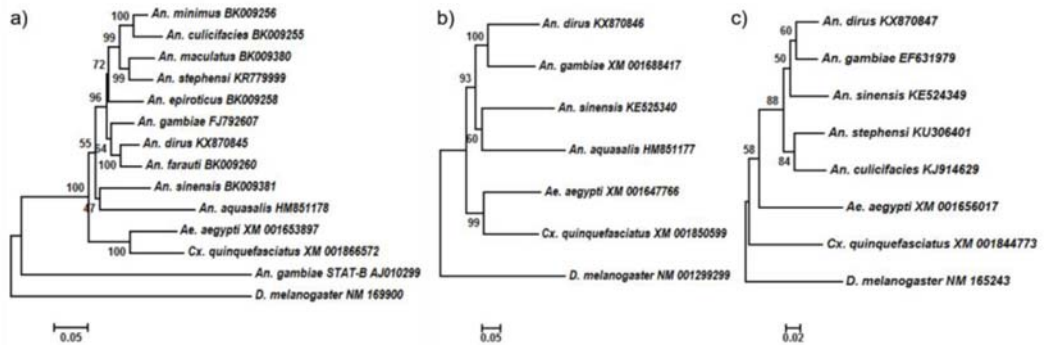

Figure 3. Phylogenetic tree of a) *STAT* gene; b) *PIAS* gene; and c) *SOCS* gene constructed from gene sequences of different mosquito species, particularly of South and Southeast Asia that are available in GenBank.The GenBank accession numbers are stated after the species names. The scale bar at the bottom are in the units of number of base substitutions per site.

3.2 *Plasmodium berghei* Infection in *An. dirus*

Oocysts and sporozoites were detected in the midgut and the salivary glands of the infected mosquitoes (Figure 4a and 4b). A substantial number of *P. berghei* oocysts were found in the guts of the infected mosquitoes and the numbers seemed to be proportionate to the density of the gametocytes in the blood meal, corroborating a study done by Sinden et al. (2007). The median number of oocysts was 280 (n=11) and 198 (n=23) when the mosquitoes were presented with a *P. berghei*-infected mouse with 0.8% and 0.43% gametocytemia, respectively (Figure 4c). It has also been found that, fully engorged females which fed on mice with parasitemia of 1.5 - 6.4%, are 100% prevalent with oocysts in their guts. A literature search shows that only two groups reported the use of the *An. dirus*/ *P. berghei* model in their experiments [21, 22]. However, these reports do not concern the development of the parasite in the mosquitoes.

The sporozoites dissected from the salivary glands of infected mosquitoes were infective, indicated by the presence of *P. berghei* parasites in the blood smear of an infected mouse on Day 5 (data not shown). These indicate that *P. berghei* is able to complete its development in *An. dirus*. This should open doors for more research on *An. dirus* disease transmission, in resource-

limited settings. *An. dirus* is naturally refractory to *P. yoelii nigeriensis* and a good understanding of the *An. dirus*/*P. yoelii* model has been achieved [23, 24].

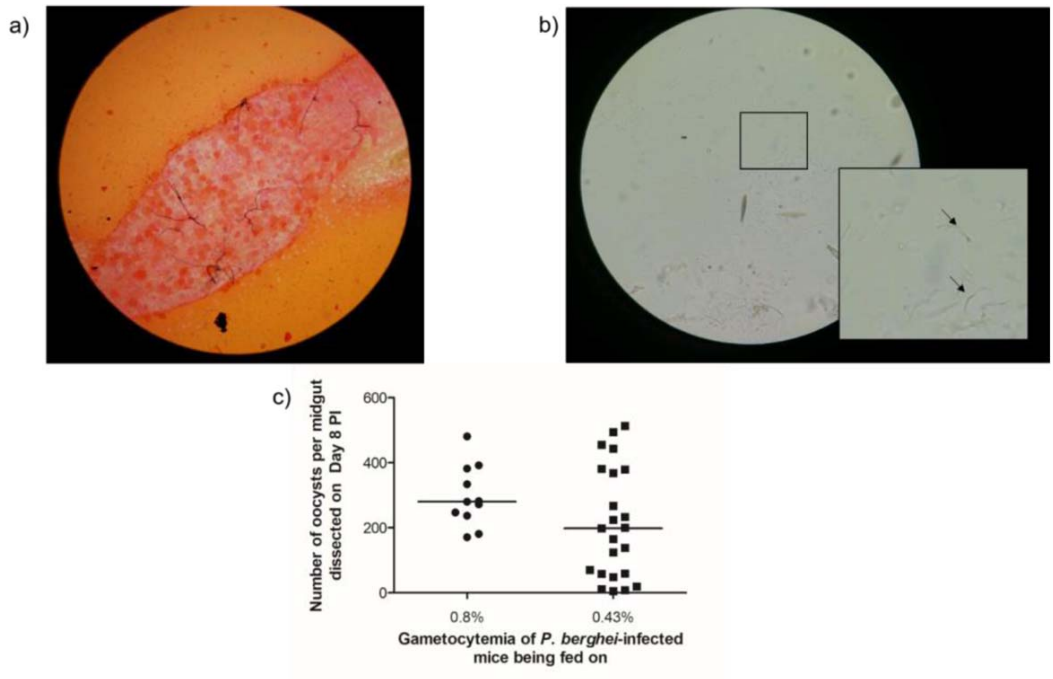

Figure 4. *P. berghei* sexual stages. a) 100 x magnification of *An. dirus* midgut with oocysts at Day 10 PI; b) 400 x magnification of *P. berghei* sporozoites at Day 20 PI; c) Oocyst counts of *An. dirus* midguts post feeding on *P. berghei*-infected mice with 0.8% (11/11 infected) and 0.43% (n=23/23 infected) gametocytemia, dissected on Day 8 PI. The dots and squares represent the number of oocysts in each midgut of *An. dirus,* which were fed on mice with 0.8% and 0.43% gametocytemia, respectively.

3.3 Time-point Gene Expression of *AdSTAT*, *AdSOCS* and *AdPIAS* Post Infection

The relative expressions of these genes are shown in Figure 5. The time points were chosen according to the developmental stages of the parasite: 12 h - ookinete; 24 h early infected stage; 48 h - early oocyst; Day 5 - intermediate oocyst stage [25]. There were no significant differences in the expression levels of the genes across the time points. The profiles barely demonstrated that *AdSTAT* and *AdSOCS* expressions seemed to peak at 24 h PI and subsequently fell, while *AdPIAS* expression appeared to be decreasing with time.

The *AdSTAT* expression profile agrees with results stating that the *STAT* gene is not transcriptionally affected, as in the *An. gambiae*/*P. berghei* model (carcass samples with midgut and ovaries removed) and *An. stephensi*/*P.berghei* model (midgut and carcass) at 24 h PI [5, 16]. Contrarily, *STAT* transcription is induced at 24 h and 36 h PI which is then no longer observed at 48 h PI in the *An. aquasalis*/*P.vivax* model [6]. It was revealed that, although no transcription of *STAT* was observed, STAT transcription factor rapidly translocates to the nucleus in the infected midguts and binds to DNA

upon *Plasmodium* infection. Nevertheless, the translocation event is not always reproducible and varies among organisms, reflecting a transient activation of STAT and the variability of the malaria infection process [17].

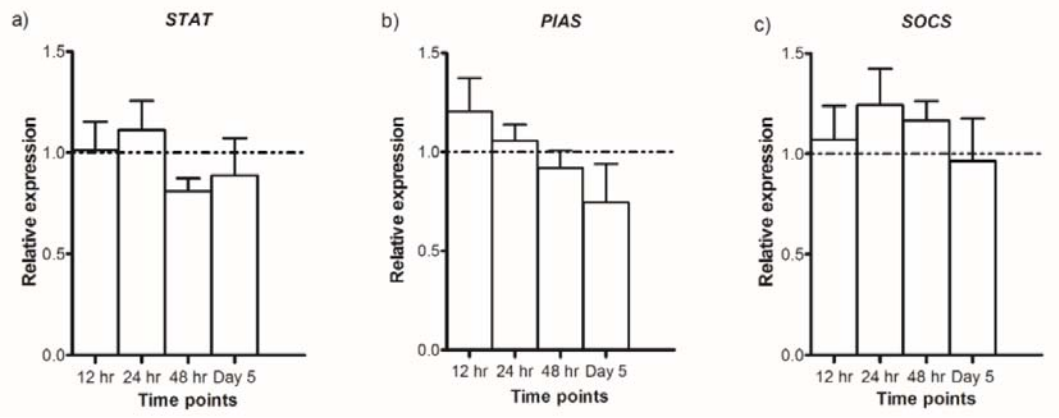

Figure 5. Time-point gene expressions (mean ± SEM) of a) *AdSTAT*; b) *AdPIAS*; and c) *AdSOCS* in *P. berghei* ANKA-infected *An. dirus*. The dotted lines at the relative expression axes indicate the expression levels of the control group (normal blood meal).

The JAK-STAT pathway is regulated by the PIAS and SOCS proteins. Thus, activation of the signaling pathway will trigger expression and activity of these negative regulators. The SOCS protein is expressed when activated by the STAT transcription factors. In this case, SOCS regulates the pathway in a negative feedback manner by inhibiting actions of the JAK kinases [26], whereas the PIAS proteins blocks DNA binding of the activated STATs through sumoylation [27]. Contrary to our results, other studies showed activation of the *Anopheles* JAK-STAT pathway during *Plasmodium* infection via induced expressions of PIAS and SOCS. *P. berghei* infection upregulates expression of *SOCS* in *An. gambiae*, *An. culicifacies* and *An. stephensi* [5, 16, 19]. Furthermore, *An. stephensi PIAS* transcripts were found to be significantly high in the infected midgut [16]. *An. aquasalis PIAS* is also transcriptionally induced at 24 h and 36 h post *P. vivax* infection [6]. The STAT pathway is activated during ookinete invasion, and the repressive proteins (SOCS and PIAS) are expressed to counter the activated pathway as a negative feedback mechanism [16, 19]. This may explain the similar trend exhibited by the *AdSTAT* and *AdSOCS* expression profiles (Figure 5).

It appears that the STAT pathway of *An. dirus* may not be induced during *P. berghei* infection, unlike the gene upregulations demonstrated in other *Anopheles*. This may indicate a no participation of the pathway during an infection in *An. dirus*. The absence of STAT-B in *An. dirus* could have contributed to the variation in function of AdSTAT, thus the result of our experiment. The addition of a second STAT may be crucial for amplification of the cascade when the pathway is activated as it was found to regulate mRNA levels of *An. gambiae* STAT-A [5]. The presence of STAT-B may have also rewired the signaling network [18]. Furthermore, it is possible that different types of mechanisms involving the STAT pathway are present [7], given the pathway's late and

early phase immune responses in the *An. gambiae*/*P. falciparum* model [5] and *An. aquasalis*/*P. vivax* model [6], respectively. Furthermore, STAT-B mRNA was found to be expressed at high levels while STAT-A was not expressed in the *An. gambiae* pupae. [5]. This indicates that STAT-B is functional and may contribute to the physiological differences among the adult Anophelines with and without STAT-B.

However, the differences in the STAT pathway expression profiles among the Anophelines, may also be caused by the different experimental setups reported. The source of extracted RNA (from different tissues) [28], infection intensity [29] and the use of different model pairs [30, 31] influence the levels of gene expressions and responses to *Plasmodium* infection in *Anopheles*. More functional assays and experiments should be performed to further confirm and understand this phenomenon in *An. dirus*. The STAT pathway is also interesting to be studied as duplicated intronless genes such as STAT often evolve new functions. These genes are also helpful in the understanding of functional and evolutionary processes in organisms.

4. CONCLUSIONS

The STAT pathway of *An. dirus* was not transcriptionally activated during *P. berghei* infection, demonstrating variation in STAT immune signaling among the mosquitoes. Further functional characterization should be carried out to validate the participation of these proteins in the immune response against *Plasmodium* infection. Studies on the STAT pathway of other *Anopheles* species will also be valuable to provide a better picture of the immunological and physiological role of this pathway. *P. berghei* ANKA was found to be able to complete its development in *An. dirus*. Studying this vector/parasite interaction laid the groundwork for further research on native *Anopheles* vectors and allows the exploitation of the newly available genome sequence of *An. dirus*, a major Southeast Asian malaria vector.

ACKNOWLEDGEMENTS

This work was funded by "Bantuan Kecil Penyelidikan" fund (BKS004-2017) and Postgraduate Research Fund (PG045-2016A) from University of Malaya.

REFERENCES

[1] Clayton A.M., Dong Y. and Dimopoulos G., *J. Innate Immun.*, 2014; **6**: 169-181. DOI 10.1159/000353602.

[2] Crompton P.D., Moebius J., Portugal S., Waisberg M., Hart G., Garver L.S., Miller L.H., Barillas-Mury C. and Pierce S.K., *Annu. Rev. Immunol.*, 2014; **32**: 157-187. DOI 10.1146/annurev-immunol-032713-120220.

[3] Zhou F. and Agaisse H., JAK/STAT Signaling and Invertebrate Immune Responses; in Decker T. and Muller M., eds., *Jak-Stat Signaling: From Basics to Disease*, Austria, 2012: 133-151.

[4] Wormald S. and Hilton D.J., *J. Biol. Chem.*, 2004; **279**: 821-824. DOI 10.1074/jbc. R300030200.

[5] Gupta L., Molina-Cruz A., Kumar S., Rodrigues J., Dixit R., Zamora R.E. and Barillas-Mury C., *Cell Host Microbe*, 2009; **5**: 498-507. DOI 10.1016/j.chom. 2009.04.003.

[6] Bahia A.C., Kubota M.S., Tempone A.J., Araujo H.R.C., Guedes B.A.M., Orfano A.S., Tadei W.P., Rios-Velasquez C.M., Han Y.S., Secundino N.F.C., Barillas-Mury C., Pimenta P.F.P. and Traub-Cseko Y.M., *PLoS Negl. Trop. Dis.*, 2011; **5**: e1317. DOI 10.1371/journal. pntd.0001317.

[7] Gupta K., Dhawan R., Kajla M., Misra

T., Kumar S. and Gupta L., *Gene*, 2017; **596**: 89-97. DOI 10.1016/j.gene.2016.09.022.

[8] Sinka M.E., Bangs M.J., Manguin S., Chareonviriyaphap T., Patil A.P., Temperley W.H., Gething P.W., Elyazar I.R., Kabaria C.W., Harbach R.E. and Hay S.I., *Parasites Vectors*, 2011; **4**: 89. DOI 10.1186/1756-3305-4-89.

[9] Sallum M.A.M., Peyton E.L. and Wilkerson R.C., *Med. Vet. Entomol.*, 2005; **19**: 158-199. DOI 10.1111/j.0269-283X.2005.00551.x

[10] Manguin S., Garros C., Dusfour I., Harbach R.E. and Coosemans M., *Infect. Genet. Evol.*, 2008; **8**: 489-503. DOI 10.1016/j.meegid.2007.11.004.

[11] Coatney G.R., Collins W.E., Warren M. and Contacos P.G., *The Primate Malarias*, U.S. Department of Health, Education and Welfare, Bethesda, 1971.

[12] Vythilingam I., Sidavong B., Chan S.T., Phonemixay T., Phetsouvanh R. and Phompida S., *Int. J. Trop. Insect Sci.*, 2005; **25**: 59-61. DOI 10.1079/IJT200554.

[13] Nakazawa S., Marchand R.P., Quang N.T., Culleton R., Manh N.D. and Maeno Y., *Int. J. Parasitol.*, 2009; **39**: 1533-1537. DOI 10.1016/j.ijpara.2009.08.005.

[14] Marchand R.P., Culleton R., Maeno Y., Quang N.T. and Nakazawa S., *Emerg. Infect. Dis.*, 2011; **17**: 1232-1239. DOI 10.3201/eid1707.101551.

[15] Khan M.B., Liew J.W.K., Leong C.S. and Lau Y.L., *Parasites Vectors*, 2016; **9**: 1-7. DOI 10.1186/s13071-016-1810-0.

[16] Gupta K., *Characterization of STAT Immune Signaling Pathway and ABC Transporters in Mosquitoes,* PhD Thesis, Birla Institute of Technology and Science Pilani, India, 2016.

[17] Barillas-Mury C., Han Y.S., Seeley D. and Kafatos F.C., *EMBO J.*, 1999; **18**: 959-967. DOI 10.1093/emboj/18.4.959.

[18] Neafsey D.E., Waterhouse R.M., Abai M.R., Aganezov S.S., Alekseyev M.A., Allen J.E., Amon J., Arca B., Arensburger P., Artemov G., Assour L.A., Basseri H., Berlin A., Birren B.W., Blandin S.A., Brockman A.I., Burkot T.R., Burt A., Chan C.S., Chauve C., Chiu J.C., Christensen M., Costantini C., Davidson V.L., Deligianni E., Dottorini T., Dritsou V., Gabriel S.B., Guelbeogo W.M., Hall A.B., Han M.V., Hlaing T., Hughes D.S., Jenkins A.M., Jiang X., Jungreis I., Kakani E.G., Kamali M., Kemppainen P., Kennedy R.C., Kirmitzoglou I.K., Koekemoer L.L., Laban N., Langridge N., Lawniczak M.K., Lirakis M., Lobo N.F., Lowy E., MacCallum R.M., Mao C., Maslen G., Mbogo C., McCarthy J., Michel K., Mitchell S.N., Moore W., Murphy K.A., Naumenko A.N., Nolan T., Novoa E.M., O'Loughlin S., Oringanje C., Oshaghi M.A., Pakpour N., Papathanos P.A., Peery A.N., Povelones M., Prakash A., Price D.P., Rajaraman A., Reimer L.J., Rinker D.C., Rokas A., Russell T.L., Sagnon N., Sharakhova M.V., Shea T., Simao F.A., Simard F., Slotman M.A., Somboon P., Stegniy V., Struchiner C.J., Thomas G.W., Tojo M., Topalis P., Tubio J.M., Unger M.F., Vontas J., Walton C., Wilding C.S., Willis J.H., Wu Y.C., Yan G., Zdobnov E.M., Zhou X., Catteruccia F., Christophides G.K., Collins F.H., Cornman R.S., Crisanti A., Donnelly M.J., Emrich S.J., Fontaine M.C., Gelbart W., Hahn M.W., Hansen I.A., Howell P.I., Kafatos F.C., Kellis M., Lawson D., Louis C., Luckhart S., Muskavitch M.A., Ribeiro J.M., Riehle M.A., Sharakhov I.V., Tu Z., Zwiebel L.J. and Besansky N.J., *Science*, 2015; **347**: 1258522. DOI 10.1126/science.1258522.

[19] Dhawan R., Gupta K., Kajla M., Kumar S., Gakhar S.K., Kakani P., Choudhury T.P. and Gupta L., *Acta Trop.*, 2015; **152**: 170-175. DOI 10.1016/j. actatropica. 2015.09.014.

[20] Sinden R.E., Dawes E.J., Alavi Y., Waldock J., Finney O., Mendoza J., Butcher G.A., Andrews L., Hill A.V., Gilbert S.C. and Basáñez M.G., *PLoS Pathog.*, 2007; **3**: e195. DOI 10.1371/ journal.ppat.0030195.

[21] Lapcharoen P., Komalamisra N., Rongsriyam Y., Wangsuphachart V., Dekumyoy P., Prachumsri J., Kajla M.K. and Paskewitz S.M., *Dev. Comp. Immunol.*, 2012; **36**: 104-111. DOI 10.1016/j.dci. 2011.06.010.

[22] Fracisco S., Gettayacamin M., Tungtaeng A., Kozar M., O'Neil M., Craft C. and Fernandes P., *Anti-malarial Activity of CEM-101, A Fluoroketolide Antimicrobial, in Both Blood Stage and Presumptive Causal Prophylactic Mouse Models*, Available at: http://www.cempra.com/common/ pdf/Posters/ASTMH%20Nov% 202010% 20FRACISCO%20CEM%20 Poster_Final% 2020101019.pdf.

[23] Somboon P., Prapanthadara L. and Suwonkerd W., *Med. Vet. Entomol.*, 1999; **13**: 355-361. DOI 10.1046/j.1365-2915. 1999.00200.x.

[24] Wang Y., Hao H., Qiu Z.W., Xu W.Y., Zhang J., Zhou T.L., Zhang X.L. and Huang F.S., *Exp. Parasitol.*, 2009; **123**: 6-10. DOI 10.1016/j.exppara.2009.05. 017.

[25] Xu X., Dong Y., Abraham E.G., Kocan A., Srinivasan P., Ghosh A.K., Sinden R.E., Ribeiro J.M.C., Jacobs-Lorena M., Kafatos F.C. and Dimopoulos G., *Mol. Biochem. Parasitol.*, 2005; **142**: 76-87. DOI 10.1016/j.molbiopara.2005.02.013.

[26] Starr R. and Hilton D.J., *BioEssays*, 1999; **21**: 47-52. DOI 10.1002/(sici)1521-1878 (199901)21:1<47::aid-bies6>3.0.co;2-n.

[27] Betz A., Lampen N., Martinek S., Young M.W. and Darnell J.E., *Proc. Nat. Acad. Sci.*, 2001; **98**: 9563-9568. DOI 10.1073/pnas.171302098.

[28] Domingos A., Pinheiro-Silva R., Couto J., do Rosário V. and de la Fuente J., *Insect Mol. Biol.*, 2017; **26**: 140-151. DOI 10.1111/imb.12289.

[29] Garver L.S., Bahia A.C., Das S., Souza-Neto J.A., Shiao J., Dong Y. and Dimopoulos G., *PLoS Pathog.*, 2012; **8**: e1002737. DOI 10.1371/journal.ppat. 1002737.

[30] Cohuet A., Osta M.A., Morlais I., Awono-Ambene P.H., Michel K., Simard F., Christophides G.K., Fontenille D. and Kafatos F.C., *EMBO Rep.*, 2006; **7**: 1285-1289. DOI 10.1038/sj.embor. 7400831.

[31] Jaramillo-Gutierrez G., Rodrigues J., Ndikuyeze G., Povelones M., Molina-Cruz A. and Barillas-Mury C., *BMC Microbiol.*, 2009; **9**: 154. DOI 10.1186/ 1471-2180-9-154